INDICATIONS FOR THE ONSET OF DECONFINEMENT IN Pb + Pb COLLISIONS AT THE CERN SPS FROM NA49*

P. Seyboth

for the NA49 Collaboration

Max–Planck–Institut für Physik, Munich, Germany

C. Alt[i], T. Anticic[u], B. Baatar[h], D. Barna[d], J. Bartke[f], L. Betev[i,j], H. Białkowska[s], C. Blume[i], B. Boimska[s], M. Botje[a], J. Bracinik[c], R. Bramm[i], R. Brun[j], P. Buncic[i,j], V. Cerny[c], P. Christakoglou[b], O. Chvala[o], J.G. Cramer[q], P. Csató[d], N. Darmenov[r], A. Dimitrov[r], P. Dinkelaker[i], V. Eckardt[n], G. Farantatos[b], D. Flierl[i], Z. Fodor[d], P. Foka[g], P. Freund[n], V. Friese[g], J. Gál[d], M. Gaździcki[i,l], G. Georgopoulos[b], E. Gładysz[f], K. Grebieszkow[t], S. Hegyi[d], C. Höhne[g], K. Kadija[u], A. Karev[n], M. Kliemant[i], S. Kniege[i], V.I. Kolesnikov[h], T. Kollegger[i], E. Kornas[f], R. Korus[l], M. Kowalski[f], I. Kraus[g], M. Kreps[c], M. van Leeuwen[a], P. Lévai[d], L. Litov[r], B. Lungwitz[i], M. Makariev[r], A.I. Malakhov[h], C. Markert[g], M. Mateev[r], B.W. Mayes[k], G.L. Melkumov[h], C. Meurer[i], A. Mischke[g], M. Mitrovski[i], J. Molnár[d], St. Mrówczyński[l], G. Pálla[d], A.D. Panagiotou[b], D. Panayotov[r], A. Petridis[b], M. Pikna[c], L. Pinsky[k], F. Pühlhofer[m], R. Renfordt[i], A. Richard[i], C. Roland[e], G. Roland[e], M. Rybczyński[l], A. Rybicki[f,j], A. Sandoval[g], H. Sann[g], N. Schmitz[n], P. Seyboth[n], F. Siklér[d], B. Sitar[c], E. Skrzypczak[t], G. Stefanek[l], R. Stock[i], H. Ströbele[i], T. Susa[u], I. Szentpétery[d], J. Sziklai[d], T.A. Trainor[q], D. Varga[d], M. Vassiliou[b], G.I. Veres[d,e], G. Vesztergombi[d], D. Vranić[g], A. Wetzler[i], Z. Włodarczyk[l], I.K. Yoo[p], J. Zaranek[i], and J. Zimányi[d]

[a]NIKHEF, Amsterdam, Netherlands
[b]Department of Physics, University of Athens, Athens, Greece
[c]Comenius University, Bratislava, Slovakia
[d]KFKI Research Institute for Particle and Nuclear Physics, Budapest, Hungary
[e]MIT, Cambridge, USA
[f]Institute of Nuclear Physics, Cracow, Poland
[g]Gesellschaft für Schwerionenforschung (GSI), Darmstadt, Germany
[h]Joint Institute for Nuclear Research, Dubna, Russia
[i]Fachbereich Physik der Universität, Frankfurt, Germany
[j]CERN, Geneva, Switzerland
[k]University of Houston, Houston, TX, USA
[l]Institute of Physics Świetokrzyska Academy, Kielce, Poland
[m]Fachbereich Physik der Universität, Marburg, Germany
[n]Max-Planck-Institut für Physik, Munich, Germany
[o]Inst. of Part. and Nuclear Physics, Charles University, Prague, Czech Rep.
[p]Department of Physics, Pusan National University, Pusan, Republic of Korea
[q]Nuclear Physics Laboratory, University of Washington, Seattle, WA, USA
[r]Atomic Physics Department, Sofia University St. Kliment Ohridski, Sofia, Bulgaria
[s]Institute for Nuclear Studies, Warsaw, Poland
[t]Institute for Experimental Physics, University of Warsaw, Warsaw, Poland
[u]Rudjer Boskovic Institute, Zagreb, Croatia

(Received October 27, 2004)

* Presented at the XXXIV International Symposium on Multiparticle Dynamics, Sonoma County, California, USA, July 26–August 1, 2004.

Particle production in central Pb+Pb collisions was studied with the NA49 large acceptance spectrometer at the CERN SPS at beam energies of 20, 30, 40, 80, and 158 GeV per nucleon. A change of the energy dependence is observed around 30A GeV for the yields of pions and strange particles as well as for the shapes of the transverse mass spectra. At present only a reaction scenario with onset of deconfinement is able to reproduce the measurements.

PACS numbers: 25.75.–q, 12.38.Mh, 12.40.Ee

1. Introduction

Qualitative considerations based on the finite size of hadrons [1] as well as quantum chromodynamics (QCD) calculations on the lattice [2, 3] predict that at sufficiently high energy density strongly interacting matter will transform into a state of quasifree quarks and gluons, the quark gluon plasma (QGP). It was also found [4] that this phase transition is of first order for finite quark masses and large non-zero baryon density. The phase boundary is predicted to end in a critical point and turn into a rapid crossover as the net baryon density decreases.

The initial phase of high energy collisions of nuclei provides the best environment to produce the deconfined phase of matter in the laboratory [5]. Lead ions first became available at the CERN SPS in 1994. It was found that in central Pb + Pb collisions at top SPS energy the initial energy density exceeds the critical value of ≈ 1 GeV/fm^3 [6]. Moreover, originally proposed signatures of the QGP were observed [7], *i.e.* J/Ψ suppression, strangeness enhancement, and possibly thermal photons and dileptons. However, these signatures are not specific for deconfinement. The NA49 collaboration therefore proposed an energy scan from 20–158A GeV in order to search for structure in the energy dependence of hadron production characteristics to provide evidence for the onset of deconfinement [8] in the lower energy range of the SPS. The measurements indeed suggest structure around 30A GeV [9] which will be discussed below.

Large event-to-event fluctuations are expected in the vicinity of the critical point. Recent predictions of its position [3] and the observed hadron production conditions indicate that collisions of lighter ions at the SPS provide a unique opportunity to study the effect of the critical point in the future.

2. Experiment NA49 at the CERN SPS

The main features of the NA49 experiment [10] are large acceptance precision tracking ($\Delta p/p^2 \approx 0.3$–7×10^{-4} (GeV/c)$^{-1}$) and particle identification using time projection chambers (TPCs). Charged particles ($\pi, K, p, \bar{p}$) are identified mostly from the measurement of their energy loss in the TPC gas (accuracy 3–6 %). Yields are obtained by fitting a sum of Gaussian functions for the various particle species to the dE/dx distributions in small bins of rapidity y and transverse momentum p_{T}. At central rapidity the identification is further improved by measurement of the time-of-flight (resolution 60 ps) to arrays of scintillation counter tiles. Strange particles (K^0_s, Λ, Ξ, Ω) are detected via decay topology and invariant mass measurement. A forward calorimeter measures the energy of the projectile spectators from which the impact parameter in $A+A$ collisions and the number of participating nucleons are deduced. NA49 also pursues an extensive program of proton induced collisions for a study of the evolution of particle production from $p+p$ via $p+$Pb to Pb + Pb reactions.

The Pb + Pb collision data presented here were taken between 1996 and 2002. For the samples at 20, 30, 40 and 80A GeV (in total about 1.5M events) the most central 7% of the inelastic cross section were selected by the online trigger. At 158A GeV two data sets with 0.8M and 3M events were recorded corresponding to the 5% and 23.5% most central reactions. Results for the upper 3 energies have been published in [9, 11] where more details on the analysis procedures may be found. Results at 20 and 30A GeV are preliminary.

3. Results

In the analysis event vertex as well as track quality cuts were applied. Particle yields were corrected for background, reconstruction efficiency, decay probability, geometric acceptance and feeddown from weak decays (for $\pi, p, \bar{p}$).

Midrapidity invariant yields as a function of the transverse mass m_{T} are shown in Fig. 1 at 158 and 20A GeV for the large variety of particle species measured by NA49. The spectra become progressively flatter with increasing particle mass, a fact that can be explained by the combined effect of the random thermal momentum distribution and strong radial flow. A "blast wave" parameterisation [12] indeed provides a reasonable description of all the spectra with two parameters: a temperature $T \approx 120$–140 MeV and a radial flow velocity of $\beta_T \approx 0.43$–0.48 c. These parameters characterize the thermal/kinetic freezeout of the fireball. The pion spectrum overshoots the model curve at low m_{T} due to the feeddown contribution from resonance decays and was therefore not used in the fit. More sophisticated model analyses [13] may indicate an earlier freezeout of the Ω and $\bar{\Omega}$ hyperons.

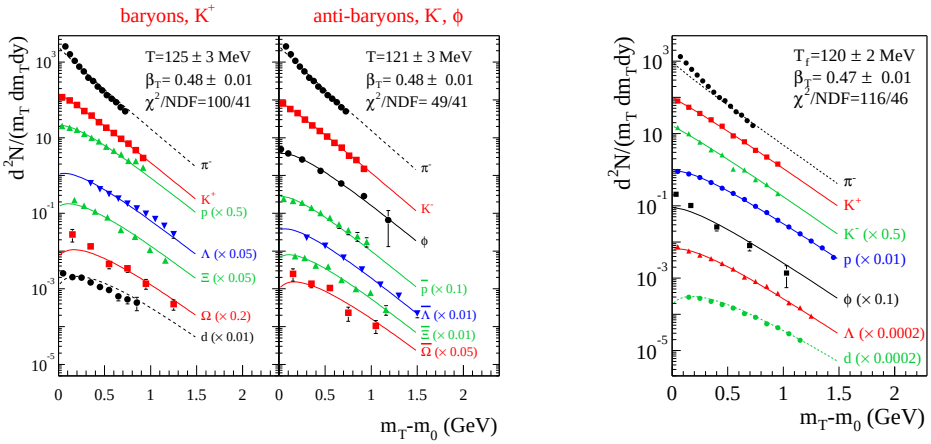

Fig. 1. Invariant yields at midrapidity in central Pb+Pb collsions at 158A (left) and 20A (right) GeV. The curves show the result of a blast wave fit [12] with parameters: temperature T and flow velocity β_T.

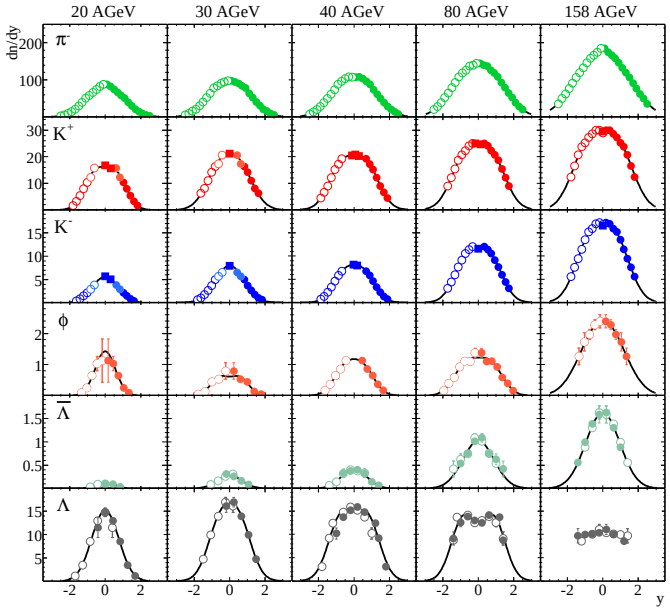

Fig. 2. Distribution of c.m.s. rapidity y for π^-, K^+, K^-, Φ, Λ and $\bar{\Lambda}$ in central Pb + Pb collisions at five SPS energies. Full (open) dots are measured (reflected), curves indicate results of single or double Gaussian fits.

The large acceptance of the NA49 detector allows measurements of rapidity spectra from midrapidity up to almost beam rapidity. Due to the symmetry of Pb + Pb collisions 4π yields can be determined. The rapidity distributions obtained by integrating the transverse momentum spectra are shown in Fig. 2 [14]. The spectra of mesons and $\bar{\Lambda}$ can be fitted by single or double Gaussians which are then used to extrapolate to 4π yields. Λ hyperons share two valence quarks with the incident nucleons and develop a wider distribution with increasing beam energy.

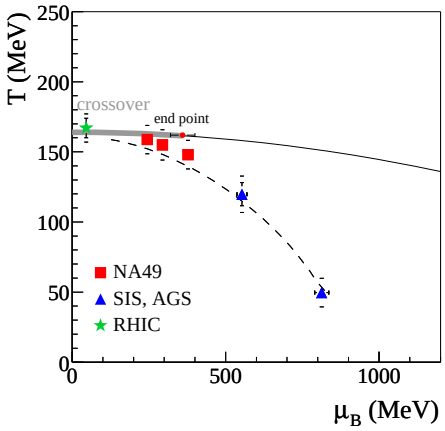

Fig. 3. Phase diagram of hadronic matter showing the hadron species freezeout points obtained from statistical model fits [16]. The dashed curve represents the empirical freezeout condition 1 GeV/hadron [15]. The line is the phase boundary between QGP and hadrons predicted by lattice QCD [3] which ends in a critical point.

Particle yields in $p+p$ and $A+A$ collisions were found to be consistent with statistical model predictions from threshold to the highest energies using only 3 parameters: a temperature T (freezeout of particle composition), a baryochemical potential μ_{B} and a strangeness suppression parameter γ_{s}. The resulting parameters T and μ_{B} [16] are plotted in the phase diagram of hadronic matter in Fig. 3 together with the phase boundary predicted by lattice QCD [3]. One observes that the freezeout points at SPS energies approach the phase boundary and the critical point.

A more detailed overview of the energy dependence of strangeness production is presented in Fig. 4. The $\langle K^+\rangle/\langle\pi^+\rangle$ ratio (upper left) shows a steep threshold rise, a maximum around the lowest SPS energy and a decrease to a somewhat lower plateau value. Although the microscopic trans-

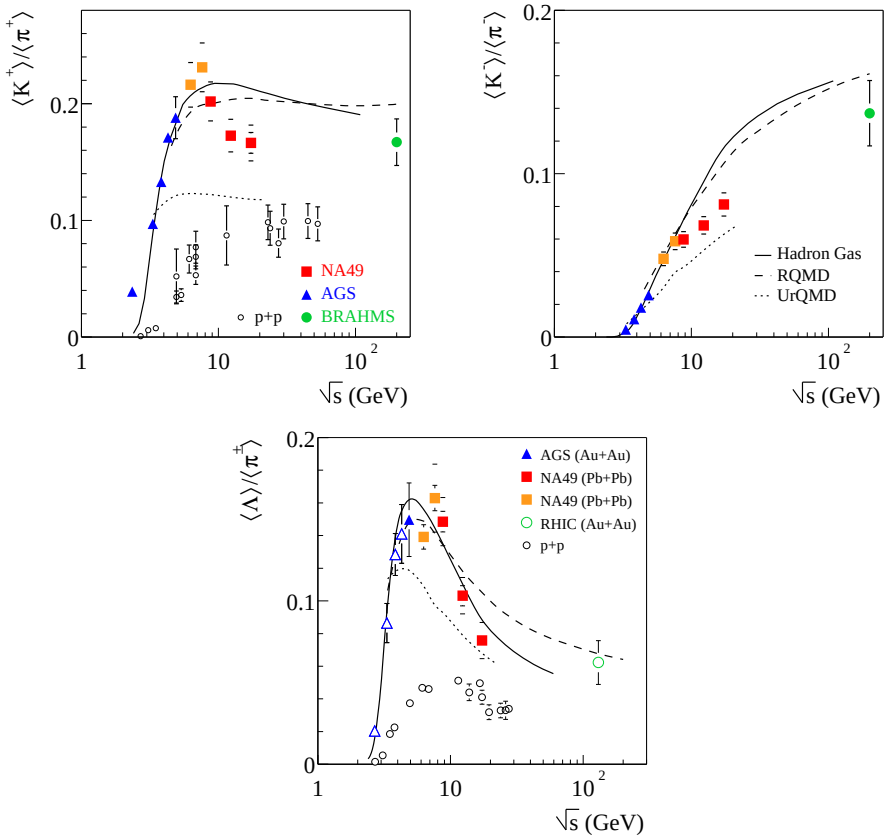

Fig. 4. Ratio of 4π yields versus energy $\sqrt{s_{NN}}$. Upper left: $\langle K^+\rangle/\langle\pi^+\rangle$. Upper right: $\langle K^-\rangle/\langle\pi^-\rangle$. Lower: $\langle\Lambda\rangle/0.5\cdot(\langle\pi^+\rangle)+(\langle\pi^-\rangle)$. Results from $p+p$ collisions (open dots) and model predictions for Pb + Pb collisions (curves) are also shown.

port models RQMD, UrQMD [17] and the statistical hadron gas model (supplemented by the freezeout condition 1 GeV/hadron [15]) follow the gross trend, they do not reproduce the pronounced peak of the strangeness/pion ratio at the SPS. Since antibaryon production yields are small, $\langle K^+\rangle$ counts essentially half of all $\bar{s}$ quarks in the final state. In contrast s quarks are distributed between anti-kaons and hyperons (mainly Λ) because of the large and decreasing net baryon density at SPS energies. The sharp peak in $\langle K^+\rangle$ is reflected in a break in the $\langle K^-\rangle/\langle\pi^-\rangle$ ratio (Fig. 4 upper right) and a wider maximum in the $\langle\Lambda\rangle/\langle\pi\rangle$ ratio (Fig. 4 lower).

The ratio of total strangeness to pion production is closely approximated by the observable $E_S=(\langle K+\bar{K}\rangle+\langle\Lambda\rangle)/\langle\pi\rangle$ which is plotted in Fig. 5 (upper left) as a function of collision energy. As expected, it shows the same sharp

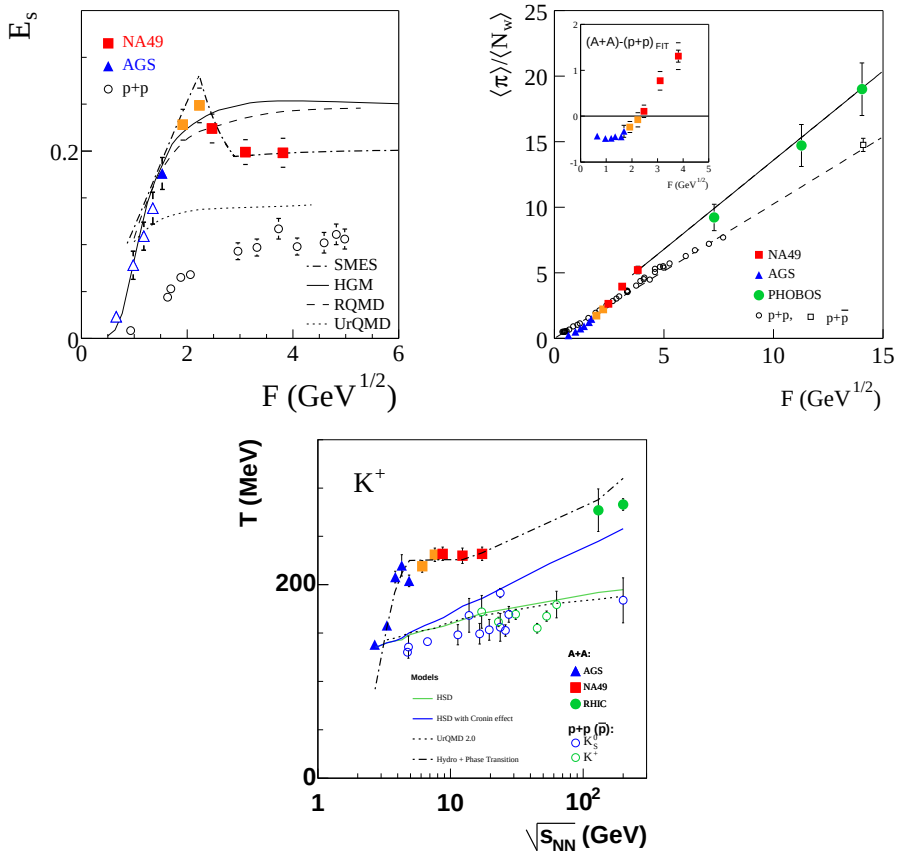

Fig. 5. Upper left: relative strangeness yields $E_S = (\langle K + \bar{K} \rangle + \langle \Lambda \rangle)/\langle \pi \rangle$ *versus* Fermi energy variable $F \approx s_{NN}^{0.25}$. Upper right: pion yield per participating nucleon $\langle \pi \rangle / \langle N_W \rangle$ *versus* F. Lower: energy dependence of the effective temperature parameter T of K^+ transverse mass spectra. Results from $p + p$ collisions are shown as open circles, model predictions for Pb + Pb collisions as curves.

peak followed by a plateau as the $\langle K^+ \rangle / \langle \pi^+ \rangle$ ratio, which is not seen in $p+p$ collisions and not reproduced by hadronic models. On the other hand this feature can be understood in a reaction scenario with the onset of deconfinement around 30A GeV as proposed in the statistical model of the early stage (SMES [8], dash-dotted curve in Fig. 5 (upper left)). E_S, a measure of the ratio of strange to nonstrange degrees of freedom in the model, drops to the value expected in the QGP. At the same energy the rate of increase of the number of produced pions per participating nucleon (a measure of the entropy per baryon in the model) was predicted to increase. As seen in

Fig. 5 (upper right), this seems to be confirmed by the measurements for collisions of heavy nuclei, while there is no change in energy dependence for $p + p$ reactions.

The invariant cross section for kaon production is well described by an exponential function $e^{-m_T/T}$. As shown in Fig. 5 (lower) for K^+ this effective temperature T rises steeply at low energies, stays at an approximately constant value through the SPS energy range and resumes a slow rise towards RHIC energy. Similar behavior is seen for the transverse spectra of K^- and pions (not shown), but is not observed in $p + p$ collisions. These features have been attributed [18] to the constant pressure and temperature when a mixed phase is present in the early stage of the reaction. In fact, a hydrodynamic calculation [19] modelling both the deconfined and the hadronic phases can provide a quantitative description (dash-dotted curve in Fig. 5 (lower)).

The NA49 detector allows for a wide range of fluctuation and correlation measurements. The event-to-event fluctuations of the K/π ratio, though small, show a slow rise with decreasing energy at the SPS. Charge fluctuations and source radii extracted from $\pi\pi$ Bose–Einstein correlations show no significant variations with energy.

4. Summary

Central Pb + Pb collisions were studied in the SPS energy range. At around 30A GeV the ratio of strangeness to pion production shows a sharp maximum, the rate of increase of the produced pion multiplicity per wounded nucleon increases and the effective temperature of pions and kaons levels to a constant value. These feature are not reproduced by present hadronic models but find a natural explanation in a reaction scenario with the onset of deconfinement in the early stage of the reaction at low SPS energy.

A considered fixed target program at RHIC and the proposed light-ion program at the SPS [20] will be able to study the role of the initial volume in the onset of deconfinement and search for evidence of the critical point of QCD in the predicted region of the phase diagram.

REFERENCES

[1] J. Collins, M. Perry, *Phys. Rev. Lett.* **34**, 1353 (1975).

[2] F. Karsch, E. Laermann, A. Peikert, *Nucl. Phys.* **B605**, 290 (2002).

[3] Z. Fodor, S. Katz, *J. High Energy Phys.* **0404**, 50 (2004).

[4] M. Stephanov, K. Rajagopal, E. Shuryak, *Phys. Rev. Lett.* **81**, 4816 (1998).

[5] See for recent results: Proceedings of Quark Matter 2004, Oakland, *J. Phys. G: Nucl. Part. Phys.* **30**, S663 (2004).

[6] T. Alber *et al.*, *Phys. Rev. Lett.* **75**, 3814 (1995).

[7] See: `http://cern.web.cern.ch/CERN/Announcements/2000/NewStateMatter/`

[8] M. Gaździcki, M.I. Gorenstein, *Acta Phys. Pol. B* **30**, 2705 (1999).

[9] S. Afanasiev *et al.*, *Phys. Rev.* **C66**, 054902 (2002); T. Anticic *et al.*, *Phys. Rev. Lett.* **93**, 022302 (2004); C. Alt *et al.*, *J. Phys. G* **30**, S119 (2004).

[10] S. Afanasiev *et al.* (NA49 Collab.), *Nucl. Instrum. Methods Phys. Res.* **A430**, 210 (1999).

[11] H. Appelshäuser *et al.*, *Phys. Lett.* **B444**, 523 (1998); T. Anticic *et al.*, *Phys. Rev. Lett.* **93**, 022302 (2004); C. Alt *et al.*, `nucl-ex/0409004`.

[12] E. Schnedermann, J. Sollfrank, U. Heinz, *Phys. Rev.* **C48**, 2462 (1993).

[13] F. Antinori *et al.*, *J. Phys. G* **30**, 823 (2004). C. Alt *et al.*, `nucl-ex/0409004`.

[14] For NA49 results at 40, 158A GeV on Ξ see: C. Meurer *et al.*, *J. Phys. G* **30**, S1325 (2004); on Ω see: C. Alt *et al.*, `nucl-ex/0409004`.

[15] J. Cleymans, K. Redlich, *Phys. Rev. Lett.* **81**, 5284 (1998).

[16] See *e.g.* F. Becattini *et al.*, *Phys. Rev.* **C69**, 024905 (2004); *J. Phys. G* **28**, 1553 (2002).

[17] RQMD: F. Wang *et al.*, *Phys. Rev.* **C61**, 064904 (2000); UrQMD: H. Weber *et al.*, *Phys. Lett.* **B545**, 285 (2002).

[18] M. Gorenstein *et al.*, *Phys. Lett.* **B567**, 175 (2003);

[19] F. Hama *et al.*, *Acta Phys. Pol. B* **35**, 179 (2004).

[20] J. Bartke *et al.*, CERN-SPSC-2003-038, SPSC-EOI-01 (2003).